

# Model-Independent Analysis of CP Violation in Charmed Meson Decays

Rohit Dhir<sup>a\*</sup>, C. S. Kim<sup>a†</sup> and Sechul Oh<sup>b‡</sup>

<sup>a</sup>*Department of Physics & IPAP, Yonsei University, Seoul 120-749, Korea*

<sup>b</sup>*University College, Yonsei University, Incheon 406-840, Korea*

## Abstract

We present a model-independent analysis of CP violation, inspired by recent experimental observations, in charmed meson decays. The topological diagram approach is used to study direct CP asymmetries for singly Cabibbo-suppressed two-body hadronic decays of charmed mesons. We extract the magnitudes and relative phases of the corresponding topological amplitudes from available experimental information. In order to get more precise and reliable estimates of direct CP asymmetries, we take into account contributions from all possible strong penguin amplitudes, including the internal  $b$ -quark penguin contributions. We also study flavor SU(3) symmetry breaking effects in these decay modes and consequently, predict direct CP asymmetries of unmeasured modes.

\* Keywords: CP violation, Asymmetry, Charm, D meson, Topological diagram, SU(3) symmetry

\* PACS numbers: 11.30.Er, 11.30.Hv, 13.25.Ft, 14.40.Lb

---

\* dhir.rohit@gmail.com

† Corresponding author, cskim@yonsei.ac.kr

‡ scohph@yonsei.ac.kr

## I. INTRODUCTION

Numerous studies of CP violation have been carried out in quark flavor physics. The  $b$ - and  $s$ -quark sectors have provided a fertile testing ground for the the standard model (SM) explanation of CP violation through the Cabibbo-Kobayashi-Maskawa (CKM) matrix. B factory experiments played a central role to confirm the CKM framework and to determine each matrix element.

In the charm sector, there are stark differences for the study of CP violation. Mixing occurs at extremely small rate in neutral charmed mesons, compared to that in neutral K and B mesons. It results in the mixing-induced indirect CP asymmetry being negligible. For direct CP violation, the asymmetry can vary greatly depending on particular charmed meson decay modes. The largest direct CP asymmetries are expected in singly Cabibbo-suppressed (SCS) decays, such as  $D^0 \rightarrow \pi^+\pi^-$  and  $D^0 \rightarrow K^+K^-$ , where interference between penguin and tree contributions can be substantial. Naturally both theoretical and experimental interest has been focused on this type of charm decays. In Cabibbo-favored (CF) decays, such as  $D^0 \rightarrow K^-\pi^+$  and  $D^+ \rightarrow \bar{K}^0\pi^+$ , the favored tree contribution dominates so that direct CP violation is negligible. In doubly Cabibbo-suppressed (DCS) decays, such as  $D^0 \rightarrow K^+\pi^-$  and  $D^+ \rightarrow K^0\pi^+$ , direct CP asymmetries are expected to be negligible in the SM, but non-negligible in certain new physics (NP) models.

Three years ago, LHCb had observed indications of direct CP asymmetry at  $3.5\sigma$  in  $\Delta a_{CP} = a_{CP}(D^0 \rightarrow K^+K^-) - a_{CP}(D^0 \rightarrow \pi^+\pi^-)$  [1]. CDF and Belle also reported similar results [2, 3], giving a world average of  $\Delta a_{CP} = (-0.678 \pm 0.147)\%$ . These results attracted great attention and led to numerous theoretical works [4–23], both in the context of the SM and of various models of NP. For a long time, direct CP violation in charm decays was expected to be below  $\mathcal{O}(10^{-3})$ . However, some of the recent studies indicate that asymmetries at  $\mathcal{O}(10^{-3})$  in these final states may not be excluded within the SM. Since then, LHCb has reported new results from which the world average has moved much closer to zero:  $\Delta a_{CP} = (-0.253 \pm 0.104)\%$  [24]. The direct CP asymmetries, reported by LHCb [25], for  $D^0 \rightarrow \pi^+\pi^-$  and  $D^0 \rightarrow K^+K^-$  are  $a_{CP}(\pi^+\pi^-) = (-0.20 \pm 0.19(\text{stat}) \pm 0.10(\text{syst}))\%$  and  $a_{CP}(K^+K^-) = (-0.06 \pm 0.15(\text{stat}) \pm 0.10(\text{syst}))\%$ . More precise measurements from future experiments, such as upgraded LHCb, BESIII and Belle II, are crucial to provide necessary information. Besides CP asymmetries, the very different experimental values of branching fractions  $\mathcal{B}(D^0 \rightarrow K^+K^-)$  and  $\mathcal{B}(D^0 \rightarrow \pi^+\pi^-)$  have been a long-standing puzzle. Some efforts have been made to resolve the issue within the SM [9, 23, 26].

For hadronic charmed meson decays, there is still no proper theoretical description of the underlying mechanism based on QCD. As well known, it is mostly because of the charm quark mass of order 1.5 GeV, which is not heavy enough to apply for a heavy quark expansion, and not sufficiently light to allow for the application of a chiral expansion. Thus, for hadronic  $D$  decays, it is not reliable to use the QCD-inspired theoretical approaches satisfactorily worked for  $B$  meson decays, such as the QCD factorization (QCDF) approach [27, 28], the perturbative QCD (pQCD) approach [29, 30] and the soft-collinear effective theory [31].

Since there is no reliable theoretical framework for hadronic decays of charmed mesons, a model-independent method, called the quark diagram approach [32–34], has been developed. In this approach all the decay amplitudes are decomposed into the so-called topological amplitudes corresponding to the different topological quark diagrams. Based on flavor SU(3) symmetry, the heavy meson decay amplitudes also can be decomposed into linear combinations of the SU(3) amplitudes which are SU(3) reduced matrix elements [35–42]. This approach is equivalent to the quark diagram approach when flavor SU(3) symmetry is imposed to the latter. Since each topological quark diagram includes all possible strong interactions to all orders, analyses of topological diagrams can provide information on final-state interactions (FSIs). In this model-independent analysis, one can determine each topological amplitude from experimental data with the help of fitting, if a sufficiently large number of measurements are available. So far several works have been done to study hadronic charmed meson decays in the framework of the quark diagram approach. However, because of the difficulty to manage the large number of parameters in fitting, those works have used at least in part certain model-dependent information (*e.g.*, information on SU(3) breaking from factorization or QCDF, etc.) to obtain a fit.

In this work we shall study direct CP asymmetries of SCS  $D_{(s)} \rightarrow PP$  ( $P = \pi, K, \eta^{(\prime)}$ ) decays using the updated experimental data. For a least model-dependent analysis of the charmed meson decays, we choose the quark diagram approach and perform the  $\chi^2$  analysis in the most general way, *i.e.*, *without using any model-dependent information*<sup>1</sup>. The present experimental data show that the measured values of branching fractions of  $D_{(s)} \rightarrow PP$  are quite accurate, but direct CP asymmetries include very large errors. In this situation our strategy is: (i) first, to fit the experimental data, especially the accurately measured branching fractions, by using the topological amplitudes as parameters, (ii) then, to extract

---

<sup>1</sup> This will be Case I of our analysis. In Case II we shall impose certain constraints on two of the parameters encouraged by the fit obtained for CF charmed meson decays.

each topological amplitude from the fit, and (iii) to make predictions for the direct CP asymmetries. Since the large number of parameters are involved in this analysis, obtaining a satisfactory fit without using any model-dependent information turns out to be a very difficult task.

We would like to emphasize that (as we shall see later) for direct CP asymmetries of SCS  $D$  decays, the penguin amplitudes corresponding to the internal  $b$ -quark (*i.e.*, internal  $b$ -quark penguin amplitudes) multiplied by the CKM factor  $V_{cb}^* V_{ub}$  become important so that it cannot be ignored. In our analysis we shall explicitly express all the relevant  $b$ -quark penguin amplitudes, including the  $b$ -penguin exchange and the  $b$ -penguin annihilation ones. Then, we shall determine the magnitudes and strong phases of these  $b$ -quark penguin amplitudes. This is one of different points of our work from the previous other works. In other words, all possible strong penguin contributions including the internal  $b$ -quark penguins are explicitly included in our analysis. We shall see that the internal  $b$ -quark penguin contributions are comparable with the internal  $s$ - and  $d$ -quark penguin ones.

This paper is organized as follows. In Sec. II, we introduce the Wolfenstein parametrization of the CKM matrix up to order  $\lambda^6$  and topological quark diagrams relevant to  $D \rightarrow PP$  decays. In Sec. III, the explicit SU(3) decomposition of the decay amplitudes and its relevance to direct CP asymmetries are presented. In Sec. IV, we perform the  $\chi^2$  analysis by taking into account SU(3) breaking to determine the topological amplitudes, and predict the direct CP asymmetries. Our conclusions are given in Sec. V.

## II. FRAMEWORK

It is well known that the Wolfenstein parametrization of the CKM matrix can be easily obtained from the standard Chau-Keung(CK) parametrization. The CKM matrix elements up to order  $\lambda^6$  are given by [43]

$$V_{\text{Wolf}}^{(\text{CK})} = \begin{pmatrix} 1 - \frac{\lambda^2}{2} - \frac{\lambda^4}{8} & \lambda & A\lambda^3(\rho - i\eta) \\ -\frac{\lambda^6}{16}[1 + 8A^2(\rho^2 + \eta^2)] & & \\ -\lambda + \frac{\lambda^5}{2}A^2(1 - 2\rho - 2i\eta) & 1 - \frac{\lambda^2}{2} - \frac{\lambda^4}{8}(1 + 4A^2) & A\lambda^2 \\ & -\frac{\lambda^6}{16}[1 - 4A^2(1 - 4\rho - 4i\eta)] & \\ A\lambda^3(1 - \rho - i\eta) & -A\lambda^2 + \frac{\lambda^4}{2}A(1 - 2\rho - 2i\eta) & 1 - \frac{\lambda^4}{2}A^2 \\ +\frac{\lambda^5}{2}A(\rho + i\eta) & +\frac{\lambda^6}{8}A & -\frac{\lambda^6}{2}A^2(\rho^2 + \eta^2) \end{pmatrix} + \mathcal{O}(\lambda^7). \quad (1)$$

Regarding charm decays, the relevant CKM factors are  $\lambda_q \equiv V_{cq}^* V_{uq}$  ( $q = d, s, b$ ). From the above matrix elements, one finds

$$\begin{aligned} \lambda_d &= -\lambda + \frac{\lambda^3}{2} + \frac{\lambda^5}{8}(1 + 4A^2) - \lambda^5 A^2(\rho + i\eta) + \mathcal{O}(\lambda^7) \equiv \lambda_d^{(1)} + \lambda_d^{(2)} + \mathcal{O}(\lambda^7), \\ \lambda_s &= \lambda - \frac{\lambda^3}{2} - \frac{\lambda^5}{8}(1 + 4A^2) + \mathcal{O}(\lambda^7), \\ \lambda_b &= \lambda^5 A^2(\rho - i\eta) + \mathcal{O}(\lambda^7) \equiv |\lambda_b|e^{-i\gamma} + \mathcal{O}(\lambda^7), \end{aligned} \quad (2)$$

where  $\lambda_d^{(1)} = -\lambda + \frac{\lambda^3}{2} + \lambda^5 \left[ \frac{1}{8} + \frac{1}{2}A^2 \right]$  and  $\lambda_d^{(2)} = -\lambda^5 A^2(\rho + i\eta) \equiv -|\lambda_d^{(2)}|e^{+i\gamma} = -|\lambda_b|e^{+i\gamma}$ . Notice that the imaginary terms appear in both  $\lambda_d$  and  $\lambda_b$  at order  $\lambda^5$ <sup>2</sup>. Thus, for CP asymmetries in charm decays, the internal  $b$ -quark contributions (penguin contributions) with the CKM factor  $\lambda_b$  as well as the  $d$ -quark ones with  $\lambda_d$  become important.

In SU(3) decomposition of the decay amplitudes for  $D \rightarrow PP$  ( $P = \pi, K, \eta^{(\prime)}$ ) modes, the decay amplitudes are expressed in terms of topological quark diagram contributions. The topological amplitudes corresponding to different topological quark diagrams, as shown in Figure 1, can be classified into three distinct groups as follows:

1. tree and penguin amplitudes:

- $\mathcal{T}$ , color-allowed tree amplitude (equivalently, external  $W$ -emission);
- $\mathcal{C}$ , color-suppressed tree amplitude (equivalently, internal  $W$ -emission);
- $\mathcal{P}$ , QCD-penguin amplitude;

---

<sup>2</sup> Note that up to order of  $\lambda^6$ ,  $\lambda_d \sim -\lambda - \lambda^5 e^{+i\gamma}$ ,  $\lambda_s \sim \lambda$ , and  $\lambda_b \sim \lambda^5 e^{-i\gamma}$ . Therefore,  $\frac{|\lambda_b|}{|\lambda_{s(d)}|} \sim \lambda^4 \sim 2 \times 10^{-3}$ .

- $\mathcal{S}$ , singlet QCD-penguin amplitude involving SU(3)-singlet mesons (e.g.,  $\eta^{(0)}$ ,  $\omega$ ,  $\phi$ );
- $\mathcal{P}_{\text{EW}}$  : color-favored EW-penguin amplitude;
- $\mathcal{P}_{\text{EW}}^{\mathcal{C}}$  : color-suppressed EW-penguin amplitude;

2. weak annihilation amplitudes:

- $\mathcal{E}$ ,  $W$ -exchange amplitude;
- $\mathcal{A}$ ,  $W$ -annihilation amplitude; ( $E$  and  $A$  are often jointly called “weak annihilation” amplitudes.)
- $\mathcal{PE}$ , QCD-penguin exchange amplitude;
- $\mathcal{PA}$ , QCD-penguin annihilation amplitude;
- $\mathcal{PE}_{\text{EW}}$  : EW-penguin exchange amplitude;
- $\mathcal{PA}_{\text{EW}}$  : EW-penguin annihilation amplitude; ( $\tilde{P}\tilde{E}$  and  $\tilde{P}\tilde{A}$  are also jointly called “weak penguin annihilation”.)

3. flavor-singlet weak annihilation amplitudes: all involving SU(3)<sub>F</sub>-singlet mesons,

- $\mathcal{SE}$ , singlet  $W$ -exchange amplitude;
- $\mathcal{SA}$ , singlet  $W$ -annihilation amplitude;
- $\mathcal{SPE}$ , singlet QCD-penguin exchange amplitude;
- $\mathcal{SPA}$ , singlet QCD-penguin annihilation amplitude;
- $\mathcal{SPE}_{\text{EW}}$  : singlet EW-penguin exchange amplitude;
- $\mathcal{SPA}_{\text{EW}}$  : singlet EW-penguin annihilation amplitude.

The reader is referred to Ref. [44] for details. Each topological quark diagram in this approach includes all possible strong interactions to all orders. Therefore, analyses of topological diagrams can provide information on final-state interactions.

### III. DECAY AMPLITUDES AND CP ASYMMETRIES

The decay amplitudes of two-body hadronic  $D$  decays can be represented in terms of the topological quark diagram contributions. In general the decay amplitudes of  $D^0 \rightarrow \pi^+\pi^-$

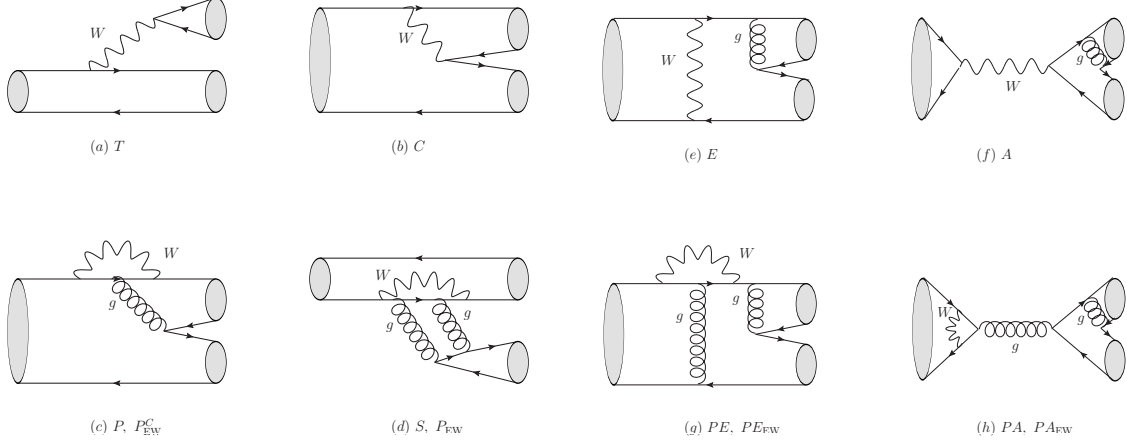


FIG. 1: Topology of possible flavor diagrams (*not* Feynman diagrams: Each topological diagram includes all possible strong interactions to all orders.): (a) color-allowed tree  $\mathcal{T}$ , (b) color-suppressed tree  $\mathcal{C}$ , (c) QCD-penguin  $\mathcal{P}$ , (d) singlet QCD-penguin  $\mathcal{S}$  diagrams, (e)  $W$ -exchange  $\mathcal{E}$ , (f)  $W$ -annihilation  $\mathcal{A}$ , (g) QCD-penguin exchange  $\mathcal{PE}$ , and (h) QCD-penguin annihilation  $\mathcal{PA}$  diagrams. The color-suppressed EW-penguin  $\mathcal{P}_{EW}^C$ , color-favored EW-penguin  $\mathcal{P}_{EW}$ , EW-penguin exchange  $\mathcal{PE}_{EW}$  and EW-penguin annihilation  $\mathcal{PA}_{EW}$  diagrams are obtained from proper replacement of gluon lines by  $Z$ -boson or photon lines in (c), (d), (g), (h), respectively.

and  $D^0 \rightarrow K^+ K^-$  can be written as

$$\begin{aligned} \mathcal{A}(D^0 \rightarrow \pi^+ \pi^-) &= \lambda_d(\mathcal{T} + \mathcal{E} + \mathcal{P}_d + \mathcal{PA}_d + \mathcal{PE}_d)^{\pi\pi} + \lambda_s(\mathcal{P}_s + \mathcal{PA}_s + \mathcal{PE}_s)^{\pi\pi} \\ &\quad + \lambda_b(\mathcal{P}_b + \mathcal{PA}_b + \mathcal{PE}_b)^{\pi\pi}; \end{aligned} \quad (3)$$

$$\begin{aligned} \mathcal{A}(D^0 \rightarrow K^+ K^-) &= \lambda_s(\mathcal{T} + \mathcal{E} + \mathcal{P}_s + \mathcal{PA}_s + \mathcal{PE}_s)^{KK} + \lambda_d(\mathcal{P}_d + \mathcal{PA}_d + \mathcal{PE}_d)^{KK} \\ &\quad + \lambda_b(\mathcal{P}_b + \mathcal{PA}_b + \mathcal{PE}_b)^{KK}, \end{aligned} \quad (4)$$

where  $\mathcal{P}_q$ ,  $\mathcal{PA}_q$ ,  $\mathcal{PE}_q$  are the QCD-penguin, QCD-penguin annihilation, QCD-penguin exchange amplitudes with an internal  $q$ -quark, respectively. Here the internal  $b$ -quark contributions with the CKM factor  $\lambda_b$  are explicitly shown.<sup>3</sup>

The possible sources of CP violation in charm transitions include: CP violation in  $\Delta C = 1$  decay amplitudes (direct CP violation) and CP violation through  $\Delta C = 2$   $D^0 - \bar{D}^0$  mixing (Indirect CP violation). The latter has been estimated to be zero in recent experiments [24].

<sup>3</sup> For simplicity, electroweak-penguin contributions have been neglected since they are expected to be very small, as previous works in the literature.

The direct CP asymmetry is defined as

$$a_{CP}(D \rightarrow f) = \frac{\mathcal{B}(D \rightarrow f) - \mathcal{B}(\bar{D} \rightarrow \bar{f})}{\mathcal{B}(D \rightarrow f) + \mathcal{B}(\bar{D} \rightarrow \bar{f})}, \quad (5)$$

where  $\mathcal{B}$  denotes a branching fraction. For  $D \rightarrow f$  decay having two strong and two weak phases, the decay amplitude can be generally written as

$$\mathcal{A}(D \rightarrow f) = |\mathcal{A}_1|e^{-i\delta_1}e^{-i\phi_1} + |\mathcal{A}_2|e^{-i\delta_2}e^{-i\phi_2}, \quad (6)$$

where  $\delta_{1,2}$  and  $\phi_{1,2}$  are strong and weak phases, respectively. Then, the direct CP asymmetry is given by

$$a_{CP}(D \rightarrow f) = \frac{2|\mathcal{A}_1||\mathcal{A}_2|\sin(\delta_1 - \delta_2)\sin(\phi_1 - \phi_2)}{|\mathcal{A}_1|^2 + |\mathcal{A}_2|^2 + 2|\mathcal{A}_1||\mathcal{A}_2|\cos(\delta_1 - \delta_2)\cos(\phi_1 - \phi_2)}, \quad (7)$$

which is non-zero only if  $\Delta\delta = \delta_1 - \delta_2 \neq 0$ ,  $\Delta\phi = \phi_1 - \phi_2 \neq 0$ , and  $|\mathcal{A}_{1,2}| \neq 0$ .

To study the direct CP asymmetry, the decay amplitude of  $D^0 \rightarrow K^+K^-$ , for instance, can be rewritten as

$$\mathcal{A}(D^0 \rightarrow \pi^+\pi^-) = \mathcal{A}_1^{\pi\pi} + \mathcal{A}_2^{\pi\pi}, \quad (8)$$

where up to order  $\lambda^6$ ,

$$\begin{aligned} \mathcal{A}_1^{\pi\pi} &= \lambda_d^{(1)}(T + Ee^{i\delta_E} + P_d e^{i\delta_P} + P A_d e^{i\delta_{PA}} + P E_d e^{i\delta_{PE}}) \\ &\quad + \lambda_s(P_s e^{i\delta_P} + P A_s e^{i\delta_{PA}} + P E_s e^{i\delta_{PE}}) \\ &\equiv |\mathcal{A}_1^{\pi\pi}|e^{-i\delta_1}, \\ \mathcal{A}_2^{\pi\pi} &= \lambda_d^{(2)}(T + Ee^{i\delta_E} + P_d e^{i\delta_P} + P A_d e^{i\delta_{PA}} + P E_d e^{i\delta_{PE}}) \\ &\quad + \lambda_b(P_b e^{i\delta_P} + P A_b e^{i\delta_{PA}} + P E_b e^{i\delta_{PE}}) \\ &= -|\lambda_d^{(2)}|(T + Ee^{i\delta_E} + P_d e^{i\delta_P} + P A_d e^{i\delta_{PA}} + P E_d e^{i\delta_{PE}})e^{+i\gamma} \\ &\quad + |\lambda_b|(P_b e^{i\delta_P} + P A_b e^{i\delta_{PA}} + P E_b e^{i\delta_{PE}})e^{-i\gamma} \\ &\equiv |\mathcal{A}_{2a}^{\pi\pi}|e^{-i\delta_2}e^{+i\gamma} + |\mathcal{A}_{2b}^{\pi\pi}|e^{-i\delta_3}e^{-i\gamma}, \end{aligned} \quad (9)$$

explicitly with the strong phases  $\delta$ 's and the weak phase  $\gamma$ , such as  $\mathcal{E} = Ee^{i\delta_E}$ . Here  $\mathcal{T}(= Te^{i\delta_T})$  is taken to be real (*i.e.*,  $\delta_T = 0$ ) and the other strong phases  $\delta$ 's are the relative ones to  $\delta_T$ . We note that the weak phase  $\gamma$  appears only in the terms having the CKM factor  $\lambda_b$  or  $\lambda_d^{(2)}$  of order  $\lambda^5$ . Thus, one expects that the direct CP asymmetry for  $D^0 \rightarrow \pi^+\pi^-$  is CKM-suppressed by the factor of  $\lambda^4 \sim 10^{-3}$ .

Within the SM, for CP asymmetries in charm decays one has to go to the CKM matrix through order  $\lambda^6$  in the Wolfenstein parametrization [45] and understand the differences



TABLE I: Topological amplitudes for  $D \rightarrow PP$  ( $P = \pi, K, \eta^{(\prime)}$ ) modes (singly Cabibbo-suppressed decays). The strong phases  $\delta$ 's and the weak phase  $\gamma$  are explicitly denoted. The CKM factor  $\lambda_d \equiv \lambda_d^{(1)} + \lambda_d^{(2)}$ , where  $\lambda_d^{(1)} = -\lambda + \frac{\lambda^3}{2} + \frac{\lambda^5}{8}(1 + 4A^2)$  and  $\lambda_d^{(2)} = -\lambda^5 A^2(\rho + i\eta) \equiv -|\lambda_2^{(2)}|e^{+i\gamma} = -|\lambda_b|e^{+i\gamma}$ . For simplicity, singlet QCD penguin, flavor-singlet weak annihilation and electroweak-penguin amplitudes have been neglected.

Mode	Representation
$D \rightarrow \pi^+ \pi^-$	$(\lambda_d^{(1)} -  \lambda_d^{(2)} e^{+i\gamma})(T + Ee^{i\delta_E} + P_d e^{i\delta_P} + PA_d e^{i\delta_{PA}} + PE_d e^{i\delta_{PE}})$ $+ \lambda_s(P_s e^{i\delta_P} + PA_s e^{i\delta_{PA}} + PE_s e^{i\delta_{PE}})$ $+  \lambda_b (P_b e^{i\delta_P} + PA_b e^{i\delta_{PA}} + PE_b e^{i\delta_{PE}})e^{-i\gamma}$
$\pi^0 \pi^0$	$\frac{1}{\sqrt{2}}[(\lambda_d^{(1)} -  \lambda_d^{(2)} e^{+i\gamma})(-Ce^{i\delta_C} + Ee^{i\delta_E} + P_d e^{i\delta_P} + PA_d e^{i\delta_{PA}} + PE_d e^{i\delta_{PE}})$ $+ \lambda_s(P_s e^{i\delta_P} + PA_s e^{i\delta_{PA}} + PE_s e^{i\delta_{PE}})$ $+  \lambda_b (P_b e^{i\delta_P} + PA_b e^{i\delta_{PA}} + PE_b e^{i\delta_{PA}})e^{-i\gamma}]$
$\pi^+ \pi^0$	$\frac{1}{\sqrt{2}}(\lambda_d^{(1)} -  \lambda_d^{(2)} e^{+i\gamma})(T + Ce^{i\delta_C})$
$K^+ K^-$	$(\lambda_d^{(1)} -  \lambda_d^{(2)} e^{+i\gamma})(P_d e^{i\delta_P} + PA_d e^{i\delta_{PA}} + PE_d e^{i\delta_{PE}})$ $+ \lambda_s(T + Ee^{i\delta_E} + P_s e^{i\delta_P} + PA_s e^{i\delta_{PA}} + PE_s e^{i\delta_{PE}})$ $+  \lambda_b (P_b e^{i\delta_P} + PA_b e^{i\delta_{PA}} + PE_b e^{i\delta_{PE}})e^{-i\gamma}$
$K^0 \bar{K}^0$	$(\lambda_d^{(1)} -  \lambda_d^{(2)} e^{+i\gamma})(Ee^{i\delta_E} + 2PA_d e^{i\delta_{PA}})$ $+ \lambda_s(Ee^{i\delta_E} + 2PA_s e^{i\delta_{PA}})$ $+  \lambda_b (2PA_b e^{i\delta_{PA}})e^{-i\gamma}$
$K^+ \bar{K}^0$	$(\lambda_d^{(1)} -  \lambda_d^{(2)} e^{+i\gamma})(Ae^{i\delta_A} + P_d e^{i\delta_P} + PE_d e^{i\delta_{PE}})$ $+ \lambda_s(T + P_s e^{i\delta_P} + PE_s e^{i\delta_{PE}})$ $+  \lambda_b (P_b e^{i\delta_P} + PE_b e^{i\delta_{PE}})e^{-i\gamma}$
$\pi^0 \eta$	$(\lambda_d^{(1)} -  \lambda_d^{(2)} e^{+i\gamma})(-Ee^{i\delta_E} + P_d e^{i\delta_P} + PE_d e^{i\delta_{PE}}) \cos \phi$ $- \lambda_s[\frac{1}{\sqrt{2}}C \sin \phi e^{i\delta_C} + (P_s e^{i\delta_P} + PE_s e^{i\delta_{PE}}) \cos \phi]$ $+  \lambda_b (P_b e^{i\delta_P} + PE_b e^{i\delta_{PE}}) \cos \phi e^{-i\gamma}$
$\pi^0 \eta'$	$(\lambda_d^{(1)} -  \lambda_d^{(2)} e^{+i\gamma})(-Ee^{i\delta_E} + P_d e^{i\delta_P} + PE_d e^{i\delta_{PE}}) \sin \phi$
$\pi^+ \eta$	$(\lambda_d^{(1)} -  \lambda_d^{(2)} e^{+i\gamma})[\frac{1}{\sqrt{2}}(T + Ce^{i\delta_C} + 2Ae^{i\delta_A}) + \sqrt{2}(P_d e^{i\delta_P} + PE_d e^{i\delta_{PE}})] \cos \phi$ $+ \lambda_s[-C \sin \phi e^{i\delta_C} + \sqrt{2}(P_s e^{i\delta_P} + PE_s e^{i\delta_{PE}}) \cos \phi]$ $+  \lambda_b [\sqrt{2}(P_b e^{i\delta_P} + PE_b e^{i\delta_{PE}})] \cos \phi e^{-i\gamma}$
$\pi^+ \eta'$	$(\lambda_d^{(1)} -  \lambda_d^{(2)} e^{+i\gamma})[\frac{1}{\sqrt{2}}(T + Ce^{i\delta_C} + 2Ae^{i\delta_A}) + \sqrt{2}(P_d e^{i\delta_P} + PE_d e^{i\delta_{PE}})] \sin \phi$ $+ \lambda_s[C \cos \phi e^{i\delta_C} + \sqrt{2}(P_s e^{i\delta_P} + PE_s e^{i\delta_{PE}}) \sin \phi]$ $+  \lambda_b [\sqrt{2}(P_b e^{i\delta_P} + PE_b e^{i\delta_{PE}})] \sin \phi e^{-i\gamma}$

TABLE II: (*Continued from Table I*) Topological amplitudes for  $D_s \rightarrow PP$  ( $P = \pi, K, \eta^{(\prime)}$ ) modes (singly Cabibbo-suppressed decays).

Mode	Representation
$D_s \rightarrow \pi^+ K^0$	$(\lambda_d^{(1)} -  \lambda_d^{(2)} e^{+i\gamma})(T + P_d e^{i\delta_P} + P E_d e^{i\delta_{PE}})$ $+ \lambda_s(Ae^{i\delta_A} + P_s e^{i\delta_P} + P E_s e^{i\delta_{PE}})$ $+  \lambda_b (P_b e^{i\delta_P} + P E_b e^{i\delta_{PE}})e^{-i\gamma}$
$K^+ \pi^0$	$\frac{1}{\sqrt{2}}(\lambda_d^{(1)} -  \lambda_d^{(2)} e^{+i\gamma})(-C e^{i\delta_C} + P_d e^{i\delta_P} + P E_d e^{i\delta_{PE}})$ $+ \lambda_s(Ae^{i\delta_A} + P_s e^{i\delta_P} + P E_s e^{i\delta_{PE}})$ $+  \lambda_b (P_b e^{i\delta_P} + P E_b e^{i\delta_{PE}})e^{-i\gamma}$
$K^+ \eta$	$(\lambda_d^{(1)} -  \lambda_d^{(2)} e^{+i\gamma})[\frac{1}{\sqrt{2}}(C e^{i\delta_C} + P_d e^{i\delta_P} + P E_d e^{i\delta_{PE}}) \cos \phi - (P_d e^{i\delta_P} + P E_d e^{i\delta_{PE}}) \sin \phi]$ $+ \lambda_s[\frac{1}{\sqrt{2}}(Ae^{i\delta_A} + P_d e^{i\delta_P} + P E_d e^{i\delta_{PE}}) \cos \phi$ $- (T + C e^{i\delta_C} + Ae^{i\delta_A} + P_s e^{i\delta_P} + P E_s e^{i\delta_{PE}}) \sin \phi]$ $+  \lambda_b (P_b e^{i\delta_P} + P E_b e^{i\delta_{PE}})(\frac{1}{\sqrt{2}} \cos \phi - \sin \phi)e^{-i\gamma}$
$K^+ \eta'$	$(\lambda_d^{(1)} -  \lambda_d^{(2)} e^{+i\gamma})[\frac{1}{\sqrt{2}}(C e^{i\delta_C} + P_d e^{i\delta_P} + P E_d e^{i\delta_{PE}}) \sin \phi + (P_d e^{i\delta_P} + P E_d e^{i\delta_{PE}}) \cos \phi]$ $+ \lambda_s[\frac{1}{\sqrt{2}}(Ae^{i\delta_A} + P_d e^{i\delta_P} + P E_d e^{i\delta_{PE}}) \sin \phi$ $+ (T + C e^{i\delta_C} + Ae^{i\delta_A} + P_s e^{i\delta_P} + P E_s e^{i\delta_{PE}}) \cos \phi]$ $+  \lambda_b (P_b e^{i\delta_P} + P E_b e^{i\delta_{PE}})(\frac{1}{\sqrt{2}} \sin \phi + \cos \phi)e^{-i\gamma}$

between other parameterizations [43]. The SM generates CP asymmetries of order  $\lambda^5$  for SCS charm decays and does not generate any CP ones for DCS decays up to order of  $\lambda^6$ .

In Table I and II, the decay amplitudes of  $D \rightarrow PP$  ( $P = \pi, K, \eta^{(\prime)}$ ) modes are expressed in terms of the topological amplitudes explicitly with the strong phases  $\delta$ 's and the weak phase  $\gamma$ . For  $D \rightarrow \pi \eta^{(\prime)}$  and  $D_s \rightarrow K \eta^{(\prime)}$  modes, the  $\eta - \eta'$  mixing is considered: in the flavor basis,

$$\begin{pmatrix} \eta \\ \eta' \end{pmatrix} = \begin{pmatrix} \cos \phi & -\sin \phi \\ \sin \phi & \cos \phi \end{pmatrix} \begin{pmatrix} \eta_q \\ \eta_s \end{pmatrix}, \quad (10)$$

where  $\eta_q = \frac{1}{\sqrt{2}}(u\bar{u} + d\bar{d})$ ,  $\eta_s = s\bar{s}$ , and the mixing angle  $\phi = 40.4^\circ$  [46].

In order to understand dynamics behind CP violation, one first needs to obtain decay amplitudes of the corresponding decays. The only model-independent way to analyze these amplitudes is to consider contributions from all possible quark diagram processes. We would like to point out that unlike all the previous works, we consider contributions from all possible strong penguin diagrams including  $b$ -quark processes. However, limited experimental

TABLE III: Experimental data for  $D \rightarrow PP$  ( $P = \pi, K, \eta^{(\prime)}$ ) modes (singly Cabibbo-suppressed decays). Branching fractions and direct CP asymmetries are shown in units of  $10^{-3}$  [24].

Mode	Expt Br ( $\times 10^{-3}$ )	Expt $a_{CP}$ ( $\times 10^{-3}$ )
$D^0 \rightarrow \pi^+ \pi^-$	$1.400 \pm 0.026$	$2.2 \pm 2.1$
$D^+ \rightarrow \pi^0 \pi^+$	$1.19 \pm 0.05$	$29.0 \pm 29.0$
$D^0 \rightarrow \pi^0 \pi^0$	$0.82 \pm 0.05$	$0.0 \pm 50.0$
$D^0 \rightarrow K^+ K^-$	$3.96 \pm 0.08$	$-2.1 \pm 1.7$
$D^+ \rightarrow \bar{K}^0 K^+$	$5.66 \pm 0.32$	$-1.1 \pm 2.5$
$D^0 \rightarrow \bar{K}^0 K^0$	$0.34 \pm 0.08$	$230 \pm 190$
$D^0 \rightarrow \pi^0 \eta$	$0.68 \pm 0.07$	—
$D^0 \rightarrow \pi^0 \eta'$	$0.89 \pm 0.14$	—
$D^+ \rightarrow \pi^+ \eta$	$3.53 \pm 0.21$	$10.0 \pm 15.0$
$D^+ \rightarrow \pi^+ \eta'$	$4.67 \pm 0.29$	$-5.0 \pm 12.0$
$D_s^+ \rightarrow K^0 \pi^+$	$2.42 \pm 0.16$	$12.0 \pm 10.0$
$D_s^+ \rightarrow K^+ \pi^0$	$0.63 \pm 0.21$	$-266 \pm 238$
$D_s^+ \rightarrow K^+ \eta$	$1.75 \pm 0.35$	$93.0 \pm 152$
$D_s^+ \rightarrow K^+ \eta'$	$1.80 \pm 0.60$	$60.0 \pm 189.0$

information and the large number of parameters to be determined has made it a rather difficult task.

#### IV. THE $\chi^2$ ANALYSIS AND SU(3) BREAKING EFFECTS

The topological amplitudes can be extracted from the available experimental information, such as branching fractions and direct CP asymmetries of SCS charm decays. Previous studies show that it is difficult to fit the experimental data in the  $\chi^2$  analysis without using additional theoretical information such as QCDF and pQCD. It is because the number of parameters in theory are large and the experimental information particularly on  $a_{CP}$  measurements in charm sector is rather poor. Also, the SU(3) breaking effects cannot be ignored, as it is impossible to fit the data within flavor SU(3) symmetry.

### A. The $\chi^2$ analysis in SU(3) limit

We perform the  $\chi^2$  analysis with 25 observables (experimental branching fractions and direct CP asymmetries) as inputs, shown in Table III. Within SU(3) symmetry, the total number of parameters is 20, including the magnitudes and strong phases of topological amplitudes, as shown in Table IV. Although the degree of freedom (d.o.f.) in this case is 5, it turns out that it is impossible to obtain a fit with an acceptable  $\chi^2/d.o.f.$  In this fit, we find  $650 \leq \chi^2/d.o.f. \leq 1000$ , being unacceptably large. This fact has also been supported by previous works based on a similar analysis [7].

### B. The $\chi^2$ analysis including SU(3) breaking effects

In order to include SU(3) breaking effects, we divide decay processes in categories of  $\pi\pi$ ,  $KK$ ,  $\pi\eta^{(\prime)}$ ,  $K\pi$  and  $K\eta^{(\prime)}$  for  $D$  and  $D_s$  decays. Then we introduce five additional parameters in their amplitudes, namely,  $\Delta_{\pi\pi}$ ,  $\Delta_{KK}$ ,  $\Delta_{\pi\eta}$ ,  $\Delta_{K\pi}$  and  $\Delta_{K\eta}$ , where each  $\Delta_{PP}$  characterizes each category of  $PP$  modes. The SU(3) broken decay amplitude in such case may, for example for  $D^0 \rightarrow \pi^+\pi^-$ , be given as

$$\begin{aligned} \mathcal{A}(D^0 \rightarrow \pi^+\pi^-) = & [(\lambda_d^{(1)} - |\lambda_d^{(2)}|e^{+i\gamma})(T + Ee^{i\delta_E} + P_d e^{i\delta_P} + PA_d e^{i\delta_{PA}} + PE_d e^{i\delta_{PE}}) \\ & + \lambda_s(P_s e^{i\delta_P} + PA_s e^{i\delta_{PA}} + PE_s e^{i\delta_{PE}}) \\ & + |\lambda_b|(P_b e^{i\delta_P} + PA_b e^{i\delta_{PA}} + PE_b e^{i\delta_{PE}})e^{-i\gamma}](1 + \Delta_{\pi\pi}). \end{aligned} \quad (11)$$

It may be noted that introduction of SU(3) breaking parameters lowers the  $\chi^2/d.o.f.$  to acceptable limits. To perform the  $\chi^2$  analysis, we use 25 observables (experimental branching fractions and direct CP asymmetries) as inputs, shown in Table III <sup>4</sup>. The total maximum number of parameters in this analysis is 24, including the magnitudes and strong phases of topological amplitudes and SU(3) breaking parameters, as shown in Table IV. Based on the choice of parameters we have two cases as follows.

#### 1. Case I: fit without any constraints

We perform a complete analysis without using any constraints to extract 24 parameters with the weak phase  $\gamma = 63^\circ$ . In this case the degree of freedom is one. The obtained

---

<sup>4</sup> The CP asymmetry of  $D^0 \rightarrow K^0 K^0$  has not been used as an input in the fit.

TABLE IV: *Case I*: Topological amplitudes and SU(3) breaking parameters determined from the fit *without any constraints*. The magnitudes and strong phases of the amplitudes are given in units of  $10^{-6}$  GeV and degrees, respectively.

No.	Parameter	Value	No.	Parameter	Value	No.	Parameter	Value
1	$T$	3.69	9	$PA_s$	1.29	17	$\delta_P$	$-144.10$
2	$C$	2.91	10	$PA_b$	1.47	18	$\delta_{PA}$	92.22
3	$A$	1.50	11	$PE_d$	0.30	19	$\delta_{PE}$	24.50
4	$E$	1.65	12	$PE_s$	2.46	20	$\Delta_{\pi\pi}$	0.006
5	$P_d$	2.18	13	$PE_b$	0.60	21	$\Delta_{K\pi}$	0.07
6	$P_s$	1.00	14	$\delta_C$	145.15	22	$\Delta_{\pi\eta}$	0.21
7	$P_b$	1.35	15	$\delta_A$	$-143.53$	23	$\Delta_{KK}$	0.011
8	$PA_d$	0.32	16	$\delta_E$	$-110.73$	24	$\Delta_{K\eta}$	0.17

numerical values of all the parameters with  $\chi^2/d.o.f. = 8.0$  are listed in Table IV <sup>5</sup>. For instance, it is found that

$$\begin{aligned} \mathcal{T} &= 3.69, & \mathcal{C} &= 2.91e^{i145.15^\circ}, \\ \mathcal{E} &= 1.65e^{-i110.73^\circ}, & \mathcal{P}_d &= 2.18e^{-i144.10^\circ}. \end{aligned} \quad (12)$$

Interestingly, the fitted values for  $\mathcal{T}, \mathcal{C}, \mathcal{E}$  are quite close to the values obtained by other works [7, 10] for analysis of *Cabibbo-favored* modes of charm decays, except for the sign of the phases <sup>6</sup>. It is noted that topological amplitudes for the internal  $b$ -quark penguin are of the same order as the  $s$ - and  $d$ -quark penguin amplitudes, though  $P_s \lesssim P_b < P_d$  <sup>7</sup>.

<sup>5</sup> The  $\chi^2/d.o.f.$  value does not seem small. However, this feature has been known in the previous works [9, 10, 26] using the similar global fit to  $D \rightarrow PP$  data. The  $\chi^2/d.o.f.$  value in the present fit mainly comes from the differences between theory fits and the central values of the poorly measured data for direct CP asymmetries. For the CP asymmetries, several modes in this fit induce sizable  $\chi^2$  values: *e.g.*, for  $D^0 \rightarrow \pi^+\pi^-$ ,  $\pi^0\pi^+$ ,  $K^+K^-$ ,  $D_s \rightarrow K^0\pi^+$ ,  $K^+\pi^0$ ,  $K^+\eta$ , the corresponding  $\chi^2$  values are 0.8, 1.0, 0.87, 1.4, 1.2, 0.8, respectively.

<sup>6</sup> In our analysis we have carefully examined the value of  $\chi^2/d.o.f.$  to determine the magnitudes and phases of the amplitudes. If the values of the phases change from the above ones, the  $\chi^2/d.o.f.$  increases.

<sup>7</sup> It may be argued that contributions from penguin amplitudes are usually expected to be considerably smaller in magnitude as compared to the color-allowed tree contribution. However, they may be enhanced due to long-distance FSI so as not to be neglected.

For  $D \rightarrow \pi\pi$ ,  $KK$  and  $D_s \rightarrow K\pi$  modes, the SU(3) breaking effects are found to be only a few percents or less. For  $D \rightarrow \pi\eta^{(\prime)}$  and  $D_s \rightarrow K\eta^{(\prime)}$  modes, the SU(3) breaking becomes as large as about 20%.

Using the fitted parameter values, the branching fractions and direct CP asymmetries are predicted, as shown in Table V. We find that the fit obtained for the branching fractions is surprisingly good (Compare Table V with Table III.). Almost all the predicted branching fractions are in very good agreement with the experimental data. It should be emphasized that the branching fractions of  $D^0 \rightarrow \pi^+\pi^-$  and  $D^0 \rightarrow K^+K^-$ , having been a long standing puzzle, are also in excellent agreement with the data. The only ambiguities in fitting arise for the  $a_{CP}$ 's of the observed decay modes which seems not to fit well in the present scenario. Since the experimental values of CP asymmetries still have very large uncertainties, in order to make a reliable conclusion, one has to wait for more precise CP measurements from the future experiments such as LHCb and Belle II. We would like to remark that to the lowest order  $a_{CP}(D \rightarrow PP)$  will include the  $b$ -quark penguin contribution multiplied by  $\sin \gamma$  (which is close to 1 for  $\gamma = 63^\circ$ ). Thus, the direct CP asymmetries of  $D \rightarrow PP$  are expected to get a significant effect from the sizable contribution of the  $b$ -quark penguin shown in Table IV.

From the fitted parameters, one can make pure predictions for direct CP asymmetries of  $D^0 \rightarrow K^0K^0$ ,  $\pi^0\eta$  and  $\pi^0\eta'$  modes which have not been used as the inputs. They are found to be

$$\begin{aligned} a_{CP}(D^0 \rightarrow \bar{K}^0K^0) &= 1.42 \times 10^{-3}, \\ a_{CP}(D^0 \rightarrow \pi^0\eta) &= 2.8 \times 10^{-4}, \\ a_{CP}(D^0 \rightarrow \pi^0\eta') &= -6.8 \times 10^{-4}. \end{aligned} \tag{13}$$

The direct CP asymmetry for  $D_s^+ \rightarrow K^+\eta$  is expected to be large, being of  $\mathcal{O}(10^{-2})$ . For  $D^0 \rightarrow \bar{K}^0K^0$  and  $D^+ \rightarrow \pi^+\eta$  modes,  $a_{CP}$ 's are expected to be of  $\mathcal{O}(10^{-3})$ . For  $D^0 \rightarrow \pi^0\pi^0$ ,  $\pi^0\eta'$ ,  $D^+ \rightarrow \bar{K}^0K^+$  and  $D_s^+ \rightarrow K^+\pi^0$  modes,  $a_{CP}$ 's are close to  $\mathcal{O}(10^{-3})$ . For the other modes including  $D^0 \rightarrow \pi^+\pi^-$ ,  $a_{CP}$ 's are of  $\mathcal{O}(10^{-4})$  or smaller. Future experimental measurements for these observables will provide useful information on this scenario.

## 2. Case II: fit with $C = 0.8T$ and $P_s = (1.0 \pm 0.2)P_d$

We put some constraints on our analysis encouraged by the fit obtained by [7] for *Cabibbo-favored* decay modes of charmed mesons. With the constraints  $C = 0.8T$  and  $P_s = (1.0 \pm 0.2)P_d$ , we obtain the fit for the remaining 22 parameters. The relation  $C = 0.8T$  holds

TABLE V: *Case I*: Branching fractions and direct CP asymmetries (in units of  $10^{-3}$ ) obtained from the fit *without any constraints*.

Mode	Br ( $\times 10^{-3}$ )	$a_{CP}$ ( $\times 10^{-3}$ )
$D^0 \rightarrow \pi^+ \pi^-$	1.40	0.30
$D^+ \rightarrow \pi^0 \pi^+$	1.19	0
$D^0 \rightarrow \pi^0 \pi^0$	0.83	0.86
$D^0 \rightarrow K^+ K^-$	3.96	-0.51
$D^+ \rightarrow \bar{K}^0 K^+$	5.68	-0.76
$D^0 \rightarrow \bar{K}^0 K^0$	0.36	1.42
$D^0 \rightarrow \pi^0 \eta$	0.68	0.28
$D^0 \rightarrow \pi^0 \eta'$	0.89	-0.68
$D^+ \rightarrow \pi^+ \eta$	3.50	1.50
$D^+ \rightarrow \pi^+ \eta'$	4.65	-1.02
$D_s^+ \rightarrow K^0 \pi^+$	2.41	0.30
$D_s^+ \rightarrow K^+ \pi^0$	0.66	-0.93
$D_s^+ \rightarrow K^+ \eta$	1.56	-42.0
$D_s^+ \rightarrow K^+ \eta'$	2.22	0.47

TABLE VI: *Case II*: Topological amplitudes and SU(3) breaking parameters determined from the fit *with*  $C = 0.8T$  and  $P_s = (1.0 \pm 0.2)P_d$ . The magnitudes and strong phases of the amplitudes are given in units of  $10^{-6}$  GeV and degrees, respectively.

No.	Parameter	Value	No.	Parameter	Value	No.	Parameter	Value
1	$T$	3.13	9	$PA_s$	1.01	17	$\delta_P$	-145.11
2	$C$	2.50	10	$PA_b$	1.48	18	$\delta_{PA}$	81.46
3	$A$	1.26	11	$PE_d$	0.52	19	$\delta_{PE}$	21.65
4	$E$	1.96	12	$PE_s$	2.42	20	$\Delta_{\pi\pi}$	0.003
5	$P_d$	1.84	13	$PE_b$	0.50	21	$\Delta_{K\pi}$	0.35
6	$P_s$	1.84	14	$\delta_C$	137.54	22	$\Delta_{\pi\eta}$	0.35
7	$P_b$	1.50	15	$\delta_A$	-159.66	23	$\Delta_{KK}$	0.33
8	$PA_d$	0.92	16	$\delta_E$	-113.50	24	$\Delta_{K\eta}$	0.32

also in the result of Case I. In this case the degree of freedom is 3. The fitted values of the parameters with  $\chi^2/d.o.f. = 9.6$  are shown in Table VI. Though the parameter values are similar to those obtained in Case I, in this case  $P_b \approx P_d = P_s$ , and the SU(3) breaking effects are as large as 32 ~ 35% for all the modes, except  $\pi\pi$  modes where the SU(3) breaking turns out to be very small.

Table VII shows the predicted branching fractions and  $a_{CP}$ 's. Here also the fit for branching fractions is excellent. As in Case I, the branching fractions of  $D^0 \rightarrow \pi^+\pi^-$  and  $D^0 \rightarrow K^+K^-$  are also in excellent agreement with the experimental data. In this case, compared with Case I, more pure predictions for direct CP asymmetries can be made. From the fitted values of the parameters, we find for  $D^0 \rightarrow \pi^+\pi^-$ ,  $K^+K^-$ ,  $\bar{K}^0K^0$ ,  $\pi^0\eta$  and  $\pi^0\eta'$  modes which have not been used as the inputs,

$$\begin{aligned}
a_{CP}(D^0 \rightarrow \pi^+\pi^-) &= 3.3 \times 10^{-4}, \\
a_{CP}(D^0 \rightarrow K^+K^-) &= -7.3 \times 10^{-4}, \\
a_{CP}(D^0 \rightarrow \bar{K}^0K^0) &= -5.8 \times 10^{-4}, \\
a_{CP}(D^0 \rightarrow \pi^0\eta) &= -4.7 \times 10^{-4}, \\
a_{CP}(D^0 \rightarrow \pi^0\eta') &= -3.3 \times 10^{-4}.
\end{aligned} \tag{14}$$

In this case, the direct CP asymmetries for several modes are expected to be smaller, compared with Case I. The direct CP asymmetries for  $D_s^+ \rightarrow K^+\pi^0$  and  $K^+\eta$  are of  $\mathcal{O}(10^{-3})$ . For  $D^0 \rightarrow \pi^0\pi^0$ ,  $K^+K^-$ ,  $D^+ \rightarrow \pi^+\eta$ ,  $\pi^+\eta'$ ,  $a_{CP}$  are close to  $\mathcal{O}(10^{-3})$ . For the other modes including  $D^0 \rightarrow \pi^+\pi^-$ ,  $a_{CP}$ 's are expected to be of  $\mathcal{O}(10^{-4})$  or smaller. Future experiments such as upgraded LHCb and Belle II will help to determine which scenario is more reliable.

## V. CONCLUSIONS

We have performed a model-independent analysis of CP violation in the singly Cabibbo-suppressed  $D \rightarrow PP$  decays. In light of the most recent CP asymmetry measurements  $a_{CP}^{\text{dir}}$  for the  $D^0 \rightarrow K^+K^-$  and  $D^0 \rightarrow \pi^+\pi^-$  modes, we have analyzed direct CP violation in  $D \rightarrow PP$  decays within the SM. It is believed that direct CP violation in such decays may arise from the interference between various topological amplitudes and the asymmetries are expected to be of  $\mathcal{O}(10^{-3})$  or smaller. We have taken advantage of the quark diagram approach to extract the topological amplitudes and relative strong phases from the measured experimental data. We have also taken care of SU(3) breaking effects which are considered to be large in these decays. It may be noted that for charmed meson decays it is difficult



TABLE VII: *Case II*: Branching fractions and direct CP asymmetries (in units of  $10^{-3}$ ) obtained from the fit *with*  $C = 0.8T$  and  $P_s = (1.0 \pm 0.2)P_d$ .

Mode	Br ( $\times 10^{-3}$ )	$a_{CP}$ ( $\times 10^{-3}$ )
$D^0 \rightarrow \pi^+\pi^-$	1.40	0.33
$D^+ \rightarrow \pi^0\pi^+$	1.18	0
$D^0 \rightarrow \pi^0\pi^0$	0.89	0.71
$D^0 \rightarrow K^+K^-$	3.98	-0.73
$D^+ \rightarrow \bar{K}^0K^+$	5.56	-0.17
$D^0 \rightarrow \bar{K}^0K^0$	0.39	-0.58
$D^0 \rightarrow \pi^0\eta$	0.68	-0.47
$D^0 \rightarrow \pi^0\eta'$	0.91	-0.33
$D^+ \rightarrow \pi^+\eta$	3.39	0.89
$D^+ \rightarrow \pi^+\eta'$	4.57	-0.67
$D_s^+ \rightarrow K^0\pi^+$	2.41	-0.15
$D_s^+ \rightarrow K^+\pi^0$	0.54	-2.43
$D_s^+ \rightarrow K^+\eta$	1.48	1.4
$D_s^+ \rightarrow K^+\eta'$	2.32	-0.23

to induce CP violation at tree level. Thus, one has to include contributions from penguin amplitudes at certain level. In order to explain the experimental branching fractions, we have included contributions from all possible strong penguin amplitudes involving penguin exchange and penguin annihilation diagrams. We have already stated that due to the large uncertainties in measured  $a_{CP}$ 's, CP violation in charmed meson decays has not yet established experimentally. This indicates that a more precise approach is needed to analyze CP violation in these decays. Therefore, we have included all the possible internal  $b$ -quark contributions to penguin diagrams (up to order of  $\lambda^6$ ) which have been ignored so far in the previous works.

In the quark diagram approach, we have determined topological amplitudes for  $D \rightarrow PP$  decays through the  $\chi^2$  analysis by using the available experimental branching fractions and direct CP asymmetries. Our  $\chi^2$  analysis has been performed in the most general way, *i.e.*, *without using any model-dependent information* on the parameters (Case I). We have divided our analysis into two cases: without any constraints (Case I) and with certain constraints (Case II), having the best  $\chi^2/d.o.f. = 8.0$  and 9.6, respectively. Consequently, we have

predicted the unmeasured direct CP asymmetries. Our findings are summarized as follows.

1. We observe an excellent fit for branching fractions, including  $\mathcal{B}(D^0 \rightarrow \pi^+\pi^-)$  and  $\mathcal{B}(D^0 \rightarrow K^+K^-)$ , in both the cases as shown in tables V and VII.
2. It may be argued that contributions from penguin amplitudes are considerably smaller in magnitude as compared to the color-allowed tree contribution. However, they may be enhanced due to long-distance FSI resonances so as not to be neglected.
3. We find that penguin contributions from the internal  $b$ -quark can be sizable and especially for CP asymmetries in charm decays, they become important and cannot be neglected.
4. Inclusion of  $b$ -quark contributions result in CP asymmetries that lies in range within the SM: *i.e.*,  $10^{-4} \leq a_{CP} \leq 10^{-3}$  for both the cases.
5. In *Case I*: (i) The observed  $\mathcal{T}, \mathcal{C}$  and  $\mathcal{E}$  acquire values closer to those found in a similar analysis based on Cabibbo-favored charm decays. The SU(3) breaking is up to 20% for  $\pi\eta^{(\prime)}$  and  $K\eta^{(\prime)}$  modes.  
(ii) We predict  $a_{CP}$ 's for  $D^0 \rightarrow \bar{K}^0 K^0 / \pi\eta / \pi\eta'$  modes to be of  $\mathcal{O}(10^{-3}) \sim \mathcal{O}(10^{-4})$ .
6. In *Case II*: (i) We use constraints  $C = 0.8T$  and  $P_s = (1.0 \pm 0.2)P_d$  to increase our predictability and to test our fit. We predict  $a_{CP}(\pi^+\pi^-) = 0.33 \times 10^{-3}$  and  $a_{CP}(K^+K^-) = -0.73 \times 10^{-3}$  with  $\Delta a_{CP} = -1.00 \times 10^{-3}$ , which are consistent with the recent experimental result.  
(ii) We also predict  $a_{CP}$ 's for  $\bar{K}^0 K^0 / \pi\eta / \pi\eta'$  modes to be of the same order of magnitude and sign.  
(iii) SU(3) symmetry breaking as large as 35% is observed in Case II for the modes other than  $\pi\pi$ .

We wish to remark here that our results are more or less comparable/consistent with other theoretical works based on similar approaches. In order to get a clearer picture, more precise experimental measurements are required to determine the exact magnitude of CP asymmetries in charmed meson decays. We hope that such an analysis would be helpful in diagnosing possible evidence of new physics in the charm sector.

\* *Note added*: When finishing the paper, we have found that two new works [22, 23] have just come out. Although those two works also use the similar approach to ours, there are

clear differences between our work and theirs. As mentioned in Introduction and Conclusions, we have performed the  $\chi^2$  analysis in the most general way, *i.e., without using any model-dependent information* on the parameters. In order to get more precise and reliable estimates of the amplitudes, we have included contributions from all possible strong penguin amplitudes, including the internal  $b$ -quark penguins. Then, we have made predictions for direct CP asymmetries of SCS  $D$  decay modes, including yet unmeasured ones.

### Acknowledgments

We thank Yeo Woong Yoon for useful comments. The work is supported by the National Research Foundation of Korea (NRF) grant funded by Korea government of the Ministry of Education, Science and Technology (MEST) (Grant No. 2011-0017430) and (Grant No. 2011-0020333).

- 
- [1] R. Aaij *et al.* [LHCb Collaboration], Phys. Rev. Lett. **108**, 111602 (2012) [arXiv:1112.0938 [hep-ex]].
  - [2] T. Aaltonen *et al.* [CDF Collaboration], Phys. Rev. Lett. **109**, 111801 (2012) [arXiv:1207.2158 [hep-ex]].
  - [3] B. R. Ko [Belle Collaboration], PoS ICHEP **2012**, 353 (2013) [arXiv:1212.1975].
  - [4] T. Feldmann, S. Nandi and A. Soni, JHEP **1206**, 007 (2012) [arXiv:1202.3795 [hep-ph]].
  - [5] J. Brod, Y. Grossman, A. L. Kagan and J. Zupan, JHEP **1210**, 161 (2012) [arXiv:1203.6659 [hep-ph]].
  - [6] J. Brod, A. L. Kagan and J. Zupan, Phys. Rev. D **86**, 014023 (2012) [arXiv:1111.5000 [hep-ph]].
  - [7] H. Y. Cheng and C. W. Chiang, Phys. Rev. D **85**, 034036 (2012) [Erratum-ibid. D **85**, 079903 (2012)] [arXiv:1201.0785 [hep-ph]].
  - [8] H. Y. Cheng and C. W. Chiang, Phys. Rev. D **86**, 014014 (2012) [arXiv:1205.0580 [hep-ph]].
  - [9] H. n. Li, C. D. Lu and F. S. Yu, Phys. Rev. D **86**, 036012 (2012) [arXiv:1203.3120 [hep-ph]].
  - [10] B. Bhattacharya, M. Gronau and J. L. Rosner, Phys. Rev. D **85**, 054014 (2012) [arXiv:1201.2351 [hep-ph]].
  - [11] E. Franco, S. Mishima and L. Silvestrini, JHEP **1205**, 140 (2012) [arXiv:1203.3131 [hep-ph]].

- [12] G. Isidori, J. F. Kamenik, Z. Ligeti and G. Perez, Phys. Lett. B **711**, 46 (2012) [arXiv:1111.4987 [hep-ph]].
- [13] Y. Grossman and D. J. Robinson, JHEP **1304**, 067 (2013) [arXiv:1211.3361 [hep-ph]].
- [14] D. Atwood and A. Soni, PTEP **2013**, no. 9, 0903B05 (2013) [arXiv:1211.1026 [hep-ph]].
- [15] G. F. Giudice, G. Isidori and P. Paradisi, JHEP **1204**, 060 (2012) [arXiv:1201.6204 [hep-ph]].
- [16] G. Hiller, Y. Hochberg and Y. Nir, Phys. Rev. D **85**, 116008 (2012) [arXiv:1204.1046 [hep-ph]].
- [17] Y. Hochberg and Y. Nir, Phys. Rev. Lett. **108**, 261601 (2012) [arXiv:1112.5268 [hep-ph]].
- [18] W. Altmannshofer, R. Primulando, C. T. Yu and F. Yu, JHEP **1204**, 049 (2012) [arXiv:1202.2866 [hep-ph]].
- [19] G. Isidori and J. F. Kamenik, Phys. Rev. Lett. **109**, 171801 (2012) [arXiv:1205.3164 [hep-ph]].
- [20] G. Hiller, M. Jung and S. Schacht, Phys. Rev. D **87**, no. 1, 014024 (2013) [arXiv:1211.3734 [hep-ph]].
- [21] F. Buccella, M. Lusignoli, A. Pugliese and P. Santorelli, Phys. Rev. D **88**, no. 7, 074011 (2013) [arXiv:1305.7343 [hep-ph]].
- [22] S. Muller, U. Nierste and S. Schacht, arXiv:1503.06759 [hep-ph].
- [23] A. Biswas, N. Sinha and G. Abbas, arXiv:1503.08176 [hep-ph].
- [24] Y. Amhis *et al.* [Heavy Flavor Averaging Group Collaboration], arXiv:1207.1158 [hep-ex].
- [25] R. Aaij *et al.* [LHCb Collaboration], JHEP **1407**, 041 (2014) [arXiv:1405.2797 [hep-ex]].
- [26] H. Y. Cheng and C. W. Chiang, Phys. Rev. D **81**, 074021 (2010) [arXiv:1001.0987 [hep-ph]].
- [27] M. Beneke, G. Buchalla, M. Neubert and C. T. Sachrajda, Nucl. Phys. B **591**, 313 (2000) [hep-ph/0006124].
- [28] M. Beneke, G. Buchalla, M. Neubert and C. T. Sachrajda, Phys. Rev. Lett. **83**, 1914 (1999) [hep-ph/9905312].
- [29] Y. Y. Keum, H. n. Li and A. I. Sanda, Phys. Lett. B **504**, 6 (2001) [hep-ph/0004004].
- [30] Y. Y. Keum, H. N. Li and A. I. Sanda, Phys. Rev. D **63**, 054008 (2001) [hep-ph/0004173].
- [31] C. W. Bauer, D. Pirjol and I. W. Stewart, Phys. Rev. D **65**, 054022 (2002) [hep-ph/0109045].
- [32] L. L. Chau, Phys. Rept. **95**, 1 (1983).
- [33] L. L. Chau and H. Y. Cheng, Phys. Rev. Lett. **56**, 1655 (1986).
- [34] L. L. Chau and H. Y. Cheng, Phys. Rev. D **36**, 137 (1987); Phys. Lett. B **222**, 285 (1989).
- [35] D. Zeppenfeld, Z. Phys. C **8**, 77 (1981).
- [36] M. J. Savage and M. B. Wise, Phys. Rev. D **39**, 3346 (1989) [Erratum-ibid. D **40**, 3127 (1989)] [Phys. Rev. D **40**, 3127 (1989)].
- [37] M. Gronau, O. F. Hernandez, D. London, J. L. Rosner, Phys. Rev. D **50**, 4529 (1994)

- [hep-ph/9404283].
- [38] M. Gronau, O. F. Hernandez, D. London and J. L. Rosner, Phys. Rev. D **52**, 6356 (1995) [hep-ph/9504326].
- [39] M. Gronau, O. F. Hernandez, D. London and J. L. Rosner, Phys. Rev. D **52**, 6374 (1995) [hep-ph/9504327].
- [40] N. G. Deshpande, X. G. He and S. Oh, Z. Phys. C **74**, 359 (1997) [arXiv:hep-ph/9511462].
- [41] S. Oh, Phys. Rev. D **60**, 034006 (1999) [arXiv:hep-ph/9812530].
- [42] X. -G. He, Eur. Phys. J. **C9**, 443-448 (1999) [hep-ph/9810397].
- [43] Y. H. Ahn, H. Y. Cheng and S. Oh, Phys. Lett. B **703**, 571 (2011) [arXiv:1106.0935 [hep-ph]].
- [44] H. Y. Cheng and S. Oh, JHEP **1109**, 024 (2011) [arXiv:1104.4144 [hep-ph]].
- [45] I. I. Bigi and A. Paul, JHEP **1203**, 021 (2012) [arXiv:1110.2862 [hep-ph]].
- [46] F. Ambrosino *et al.*, JHEP **0907**, 105 (2009) [arXiv:0906.3819 [hep-ph]].